

Switching Current *vs.* Magnetoresistance in Magnetic Multilayer Nanopillars.

S. Urazhdin, Norman O. Birge, W. P. Pratt Jr., and J. Bass

Department of Physics and Astronomy, Center for Fundamental Materials Research and Center for Sensor Materials, Michigan State University, East Lansing, MI 48824

We study current-driven magnetization switching in nanofabricated magnetic trilayers, varying the magnetoresistance in three different ways. First, we insert a strongly spin-scattering layer between the magnetic trilayer and one of the electrodes, giving increased magnetoresistance. Second, we insert a spacer with a short spin-diffusion length between the magnetic layers, decreasing the magnetoresistance. Third, we vary the angle between layer magnetizations. In all cases, we find an approximately linear dependence between magnetoresistance and inverse switching current. We give a qualitative explanation for the observed behaviors, and suggest some ways in which the switching currents may be reduced.

PACS numbers: 73.40.-c, 75.60.Jk, 75.70.Cn

The observation [1] of predicted [2, 3] current-driven switching in nanofabricated magnetic multilayers (nanopillars) opened the possibility for direct switching of the bits in magnetic memory by local application of current, rather than by the field of external wires. However, the present switching currents I_s are too large for high-density applications. In this paper, we describe three new experiments that show an approximately linear dependence between $1/I_s$ and the change of resistance ΔR upon switching. These results should provide guidance for both theory and engineering of current-switching devices.

First, we enhance ΔR in Py/Cu/Py/Cu (Py=Permalloy= $\text{Ni}_{84}\text{Fe}_{16}$) trilayer nanopillars by inserting 1 nm of a strong spin-scatterer, $\text{Fe}_{50}\text{Mn}_{50}$ [4] between the trilayer and the top electrode. Second, we insert a t_{CuPt} thick $\text{Cu}_{96}\text{Pt}_6$ layer between the Py layers. The short spin-diffusion length in $\text{Cu}_{94}\text{Pt}_6$ decreases ΔR . Third, we study ΔR and the switching currents I_s as a function of the angle between the magnetizations of the two ferromagnetic layers in Py/Cu/Py nanopillars.

Our samples were made with a multistep process described elsewhere [5]. Below, all thicknesses are in nm. The basic samples had structure $\text{Cu}(80)/\text{F}_1=\text{Py}(30)/\text{N}(15)/\text{F}_2=\text{Py}(6)/\text{Cu}(2)/\text{Au}(150)$. The bottom $\text{Cu}(80)/\text{Py}(30)$ layers were extended leads,

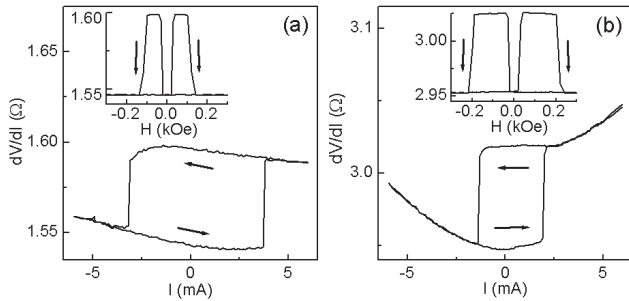


FIG. 1: (a) dV/dI vs. I for a sample of type 1 (as defined in the text) at $H = 0$. Inset: dV/dI vs. H at $I = 0$. (b) Same as (a), for a sample of type 2.

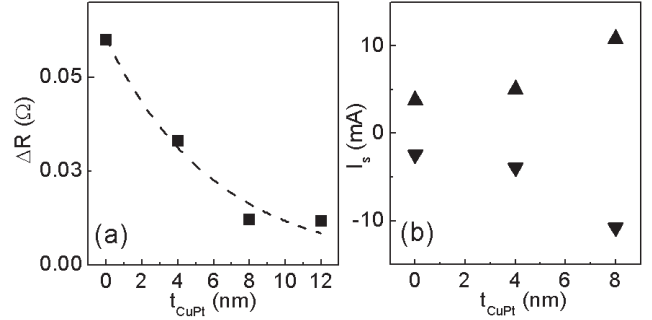


FIG. 2: (a) Variation of ΔR with t_{CuPt} . Dashed line is a fit with $\Delta R = \Delta R_0 \exp[-t_{\text{CuPt}}/l_{\text{sf}}^{\text{CuPt}}]$, $\Delta R_0 = 0.06 \pm 0.004 \Omega$, $l_{\text{sf}}^{\text{CuPt}} = 6.1 \pm 0.8$ nm. (b) $I_s^{P \rightarrow AP}$ (upward triangles) and $I_s^{AP \rightarrow P}$ (downward triangles) vs. t_{CuPt} .

N, F₂ and Cu(2) were patterned into an elongated shape with dimensions $\approx 130 \times 70$ nm, and Au(150) was the top lead. Leaving F₁ extended minimizes the effect of dipolar coupling on the current-driven switching [6]. N was $\text{Cu}(13.5\text{-d})/\text{Cu}_{94}\text{Pt}_6(\text{d})/\text{Cu}(1.5)$, with $d=0, 0, 4, 8, 12$ in sample types 1 through 5, respectively. In sample type 2, the Cu(2) layer was replaced with a $\text{Cu}(2)/\text{Fe}_{50}\text{Mn}_{50}(1)/\text{Cu}(2)$ sandwich. We measured dV/dI at room temperature (295 K) with four-probes and lock-in detection, adding an ac current of amplitude 20–40 μA at 8 kHz to the dc current I . At least 7 samples of each type were tested. Typical sample resistances were 1 to 3 Ω . Variations in resistances are attributed to scatter in both nanopillar sizes and contact resistances to the electrodes. Positive current flows from the extended to the patterned Py layer. H is in the film plane and (except for the angular dependence studies) along the nanopillar easy axis.

Fig. 1 compares typical results for a sample of type 1 (Fig. 1(a)) vs. a sample of type 2, (Fig. 1(b)). In both cases, negative current I leads to transition from the antiparallel (AP) state with high resistance R_{AP} to the parallel (P) state with low resistance R_P at $I = I_s^{AP \rightarrow P}$. A reverse transition occurs at positive $I = I_s^{P \rightarrow AP}$. In the

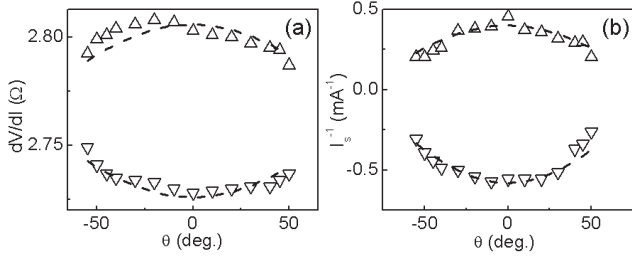


FIG. 3: (a) Quasi-parallel (P) and quasi-antiparallel (AP) state resistances R_P (upward triangles) and R_{AP} (downward triangles) vs. θ . Dashed curves: fits with $R_{P,AP} = R_0 \mp A \cos \theta$, $R_0 = 2.77 \Omega$, $A = 0.04 \Omega$. (b) $1/I_s^{P \rightarrow AP}$ (upward triangles) and $1/I_s^{AP \rightarrow P}$ (downward triangles) vs. θ . Dashed curves: fits with $1/I_s^{P \rightarrow AP, AP \rightarrow P} = K_{P,AP} \cos \theta$, $K_P = 0.40 \text{ mA}^{-1}$, $K_{AP} = -0.58 \text{ mA}^{-1}$.

H sweep at $I = 0$ (insets Fig. 1(a,b)), the extended F_1 layer reverses at $H \approx 20$ Oe, and F_2 reverses at the field $H_s \approx 100 - 200$ Oe, determined by the shape anisotropy of F_2 . The average H_s in samples of type 1 and type 2 were similar, insets of Fig. 1 only illustrate scatter among samples. There was no systematic correlation between I_s and H_s . Since the high resistivity $\rho \approx 100 \mu\Omega\text{cm}$ of $\text{Fe}_{50}\text{Mn}_{50}$ contributes only $\approx 0.25 \Omega$ to the resistance of samples of type 2, the contact resistance in Fig. 1(b) must be $\approx 1 \Omega$ larger than that in Fig. 1(a). For 14 samples of type 1, $\Delta R \equiv R_{AP} - R_P = 0.060 \pm 0.002 \Omega$, $I_s^{AP \rightarrow P} = -2.45 \pm 0.2 \text{ mA}$, and $I_s^{P \rightarrow AP} = 3.8 \pm 0.2 \text{ mA}$. For 12 samples of type 2, $\Delta R = 0.085 \pm 0.012 \Omega$, $I_s^{AP \rightarrow P} = -1.5 \pm 0.2 \text{ mA}$, and $I_s^{P \rightarrow AP} = 1.85 \pm 0.2 \text{ mA}$. For uncertainties, we give twice the standard deviations of the mean. The main result of this experiment is the higher ΔR , and lower I_s , in the nanopillars with the inserted $\text{Fe}_{50}\text{Mn}_{50}(1)$ layer.

Fig. 2 shows data for sample types 1, 3, 4, 5. Fig. 2(a) ($\Delta R(t_{\text{CuPt}})$) gives a spin-diffusion length of $6.1 \pm 0.8 \text{ nm}$ in $\text{Cu}_{94}\text{Pt}_6$ at 295 K, shorter than $\approx 10 \text{ nm}$ at 4.2 K [4]. Fig. 2(b) shows that both $I_s^{P \rightarrow AP}$ and $|I_s^{AP \rightarrow P}|$ increase with increasing t_{CuPt} . Interestingly, the ratio $I_s^{P \rightarrow AP}/|I_s^{AP \rightarrow P}|$ decreases from ≈ 1.5 at $t_{\text{CuPt}} = 0$ to ≈ 1.0 for $t_{\text{CuPt}} = 8$. This decrease with increase of spin-flipping within the N-layer is opposite to that reported in [7] for a similar measurement with varied thickness of $\text{N}=\text{Cu}$, and is inconsistent with the explanation proposed there. All 8 samples of type 5 showed hysteretic field-driven switching, similar to other sample types. However, none showed reproducible hysteretic current-switching. Such a qualitative change at sufficiently large t_{CuPt} is expected. When the Py layers are nearly decoupled due to spin-flip scattering in a thick $\text{Cu}_{94}\text{Pt}_6$ layer, the effect of current becomes independent of the mutual orientations of these layers. This effect is similar to that for a single magnetic layer, and cannot lead to hysteretic switching between P and AP states.

Fig. 3 shows the results for varied non-collinear orientations of magnetic layers in sample type 1. Before

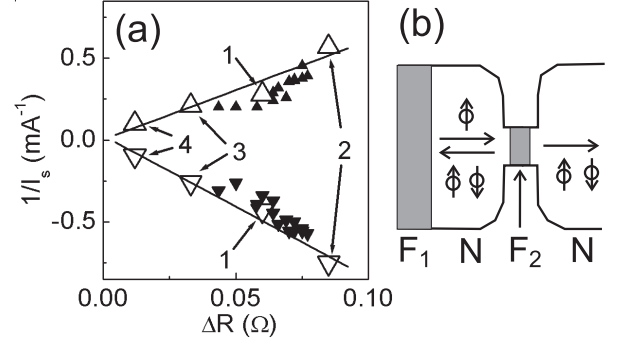


FIG. 4: (a) Dependence of $1/I_s^{P \rightarrow AP}$ (upward triangles) and $1/I_s^{AP \rightarrow P}$ (downward triangles) on ΔR . Open symbols: sample types 1 through 4, as labeled. Solid symbols: variations with angle between the magnetizations in a sample of type 1. Solid lines: best linear fits of data, excluding the angular dependence. The ordinate intercepts are zero within the uncertainty of the fits, (b) Schematic of electron scattering in nanopillar, as discussed in the text.

each measurement, a pulse of $H = 60$ Oe at the desired in-plane angle θ was applied to rotate the magnetization M_1 of F_1 parallel to H , then the current-switching was measured at $H = 10$ Oe, needed to fix M_1 . The data in Fig. 3 confirm results reported in [8], but with a larger magnetoresistance $\Delta R/R$.

In Fig. 4(a) we collect together the data of Figs. 1-3 in a plot of average values of $1/I_s$ vs. average ΔR . The variations among different samples lead to uncertainties of the average values, close to the symbol sizes in Fig. 4(a). The overall agreement of the data for three different types of measurements suggests a general inverse relationship between I_s and ΔR , independent of the particular way in which ΔR was varied. The switching is determined by the current density, so both $1/I_s$ and ΔR are inversely proportional to the nanopillar areas; their variation only leads to scaling along the approximately linear dependence in Fig. 4(a).

To qualitatively describe the inverse relationship in Fig. 4(a), we use the simplest plausible ballistic model, in which the electrons polarized by F_1 are scattered in F_2 , generating magnetic excitations. Fig. 4(b) shows a cartoon of this model, where a spin-up electron coming from F_1 is either transmitted or reflected by F_2 . In either case, it can flip its spin, exciting (or de-exciting) the F_2 layer. We introduce a parameter p , describing the polarization of current if F_2 is removed. We define the sign of p with respect to the direction of magnetization M_2 of F_2 . For Py (sample type 1), we expect $p \approx 0.45 - 0.6$ [9, 10]. When F_1 is absent, $p = 0$. The current polarization in the diffusive transport model [11] is different; it depends both on F_1 and F_2 , and does not disappear when F_1 is absent.

In our model, ΔR is determined by the spin-dependent resistance of the interfaces and bulk of F_2 and is proportional to p . We can interpret the variations of ΔR in terms of a change in polarization p . When

$\text{Cu}_{94}\text{Pt}_6$ is inserted between F_1 and F_2 , spin-flip scattering in this layer decreases p according to $p(t_{\text{CuPt}}) = p(0)\exp[-t_{\text{CuPt}}/l_{sf}^{\text{CuPt}}]$, consistent with Fig. 2(a). The angular dependence of Fig. 3(a) can be understood similarly in terms of the projection of spin current onto the direction of the magnetization of F_2 , giving $p(\theta) = p(0)\cos(\theta)$. Finally, the $\text{Fe}_{50}\text{Mn}_{50}$ inserts outside F_2 have very short spin-diffusion length. Although the resulting increase of MR involves spin-diffusion outside the magnetic trilayer, and cannot be described by our ballistic model, it is also reasonable to approximate the effect of the $\text{Fe}_{50}\text{Mn}_{50}$ inserts as an increase of p .

The current-driven switching is also expected to be determined by p . Electrons with spin opposite to M_2 can generate magnetic excitations when they flip their spins, while electrons with spins along the magnetization can absorb the excitation when they spin-flip, as follows from the conservation of angular momentum along M_2 [3]. Thus, we may expect the rate of magnetic excitation by current to be given by the difference between the spin-down and spin-up electron currents, i.e. approximately proportional to $p \cdot I$. $p \cdot I_s$ is then determined by the level of magnetic excitation, needed for the magnetization switching, i.e. $1/I_s \propto p$. The data and linear fits (solid lines) in Fig. 4(a) are consistent with this analysis. Our data are also generally consistent with the more quantitative analyses of current-driven switching based on the popular spin-torque model [2, 11], and the recently proposed effective temperature model [12]. These

models differ from each other in details, which need further experimental testing.

Our data, and the simple model, suggest that one might reduce I_s by using a more highly polarizing ferromagnet for F_1 , or by being more clever in designing the layers 'outside' the $F_1/\text{N}/F_2$ trilayer. Independent evidence that the current-driven switching is determined by the N/F_2 interfaces [7] suggests that modifying those interfaces (e.g. by varying their roughness or local composition) should be worth exploring. At room temperature, the current-driven switching is thermally activated [13, 14]. An obvious way of decreasing the switching current is then to lower the switching barrier. But a smaller switching barrier also leads to thermal activation at room temperature without applied current, thus reducing the effectiveness of the nanopillars for information storage.

To summarize, we measured the changes in resistance upon switching, ΔR , and the switching currents, I_s , in Permalloy (Py)-based trilayer nanopillars with: a) strong spin flipping between the nanopillar and one of the leads, b) spin-flipping in the spacer between the Py layers, c) varying angle between the magnetizations of the Py layers. We find a linear relation between I_s^{-1} and ΔR . We describe the data in terms of a qualitative ballistic model.

This work was supported by the MSU CFMR, CSM, the MSU Keck Microfabrication facility, the NSF through Grants DMR 02-02476, 98-09688, and NSF-EU 00-98803, and Seagate Technology.

-
- [1] J.A. Katine, F.J. Albert, R.A. Buhrman, E.B. Myers and D.C. Ralph, Phys. Rev. Lett. **84**, 3149 (2000), and references in J. Bass, S. Urazhdin, N.O. Birge, and W.P. Pratt Jr., Phys. Stat. Sol. (in press).
- [2] J. Slonczewski, J. Magn. Magn. Mater. **159**, L1 (1996).
- [3] L. Berger, Phys. Rev. **B 54**, 9353 (1996).
- [4] W. Park, D.V. Baxter, S. Steenwyk, I. Moraru, W.P. Pratt Jr., and J. Bass, Phys. Rev. **B 62**, 1178 (2000).
- [5] S. Urazhdin, H. Kurt, W.P. Pratt Jr., and J. Bass, Appl. Phys. Lett. **83**, 114 (2003).
- [6] F. J. Albert, J.A. Katine, R.A. Buhrman, and D.C. Ralph, Appl. Phys. Lett. **77**, 3809 (2000).
- [7] F. J. Albert, N.C. Emley, E.B. Myers, D.C. Ralph, and R.A. Buhrman, Phys. Rev. Lett. **89**, 226802 (2002).
- [8] F.B. Mancoff, R.W. Dave, N.D. Rizzo, T.C. Eschrich, B.N. Engel, and S. Tehrani, Appl. Phys. Lett. **83**, 1596 (2003).
- [9] W. P. Pratt Jr., S.D. Steenwyk, S.Y. Chiang, A.C. Scafer, R. Loloee, and J. Bass, IEEE Trans. Magn. **33**, 3505 (1997).
- [10] B. Nadgorny, R.J. Soulen Jr., M.S. Osofsky, I.I. Mazin, G. Laparade, R.J.M. van de Veerdonk, A.A. Smits, S.F. Cheng, E.F. Skelton, and S.B. Qadri, Phys. Rev. **B 61**, R3788 (2000).
- [11] A.A. Kovalev, A. Brataas, and G.E.W. Bauer, Phys. Rev. **B 66**, 224424 (2002).
- [12] S. Urazhdin, cond-mat/0308320.
- [13] E. B. Myers, F.J. Albert, J.C. Sankey, E. Bonet, R.A. Buhrman, and D.C. Ralph, Phys. Rev. Lett. **89**, 196801 (2002).
- [14] S. Urazhdin, N.O. Birge, W.P. Pratt Jr., and J. Bass, Phys. Rev. Lett. (in press), cond-mat/0303149.